AD-A188 462 LASER RAMAN STUDIES RELATED TO LIQUID PROPELLANTS: STRUCTURAL CHARACTERIS..(U) ARMY BALLISTIC RESEARCH LAB ABERDEEN PROVING GROUND MD J A VANDERHOFF ET AL. 1/1

UNCLASSIFIED AUG 87 BRL-TR-2845 F/G 19/1 NL

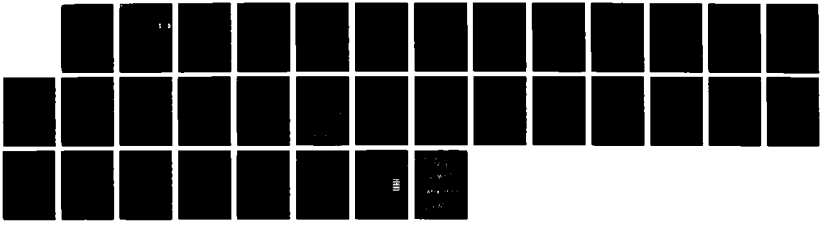

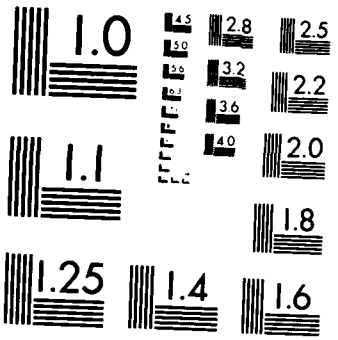

AD

TECHNICAL REPORT BRL-TR-2845

LASER RAMAN STUDIES RELATED TO LIQUID PROPELLANTS: STRUCTURAL CHARACTERISTICS INFERRED FROM THE NITRATE ANION SPECTRA

JOHN A. VANDERHOFF
STEVEN W. BUNTE
PHILIP M. DONMOYER

AUGUST 1987

US ARMY BALLISTIC RESEARCH LABORATORY
ABERDEEN PROVING GROUND, MARYLAND

DESTRUCTION NOTICE

Destroy this report when it is no longer needed. DO NOT return it to the originator.

Additional copies of this report may be obtained from the National Technical Information Service, U.S. Department of Commerce, Springfield, VA 22161.

The findings of this report are not to be construed as an official Department of the Army position, unless so designated by other authorized documents.

The use of trade names or manufacturers' names in this report does not constitute indorsement of any commercial product.

UNCLASSIFIED
SECURITY CLASSIFICATION OF THIS PAGE

REPORT DOCUMENTATION PAGE

Form Approved
OMB No 0704-0188
Exp Date Jun 30, 1986

1a. REPORT SECURITY CLASSIFICATION Unclassified	1b. RESTRICTIVE MARKINGS
2a. SECURITY CLASSIFICATION AUTHORITY	3. DISTRIBUTION/AVAILABILITY OF REPORT
2b. DECLASSIFICATION/DOWNGRADING SCHEDULE	
4. PERFORMING ORGANIZATION REPORT NUMBER(S) BRL-TR-2845	5. MONITORING ORGANIZATION REPORT NUMBER(S)
6a. NAME OF PERFORMING ORGANIZATION US Army Ballistic Research Laboratory 6b. OFFICE SYMBOL (If applicable) SLCBR-IB	7a. NAME OF MONITORING ORGANIZATION
6c. ADDRESS (City, State, and ZIP Code) Aberdeen Proving Ground, MD 21005-5066	7b. ADDRESS (City, State, and ZIP Code)
8a. NAME OF FUNDING/SPONSORING ORGANIZATION 8b. OFFICE SYMBOL (If applicable)	9. PROCUREMENT INSTRUMENT IDENTIFICATION NUMBER
8c. ADDRESS (City, State, and ZIP Code)	10. SOURCE OF FUNDING NUMBERS PROGRAM ELEMENT NO. 61102A; PROJECT NO. AH43; TASK NO.; WORK UNIT ACCESSION NO.

11. TITLE (Include Security Classification)
LASER RAMAN STUDIES RELATED TO LIQUID PROPELLANTS: STRUCTURAL CHARACTERISTICS INFERRED FROM THE NITRATE ANION SPECTRA

12. PERSONAL AUTHOR(S)
John A. Vanderhoff, Steven W. Bunte, and Philip M. Donmoyer

13a. TYPE OF REPORT	13b. TIME COVERED	14. DATE OF REPORT (Year, Month, Day)	15. PAGE COUNT
Final	FROM Jun 86 TO Sep 86		

16. SUPPLEMENTARY NOTATION

17. COSATI CODES		
FIELD	GROUP	SUB-GROUP
07	04	

18. SUBJECT TERMS (Continue on reverse if necessary and identify by block number)
HAN, Laser Raman Spectroscopy, Nitrate Anion, Liquid Propellants

19. ABSTRACT (Continue on reverse if necessary and identify by block number)

Experimental Raman studies on aqueous hydroxylammonium nitrate (HAN) show concentration dependent center frequency and linewidth changes of the NO_3^- vibrations which are similar to the aqueous alkali-metal nitrates; but not ammonium nitrate. Comparison of Raman spectra for HAN and silver nitrate dissolved in both water and acetonitrile demonstrate there is no substantial contact-ion pairing for aqueous HAN solutions at concentrations around 0.2 M. Markedly decreased linewidths and band splittings occur when HAN is solidified. The center frequency of the Raman bands have been observed to be temperature dependent. From -50°C to 22°C, the ν_4 band center frequency decreases by about 4/cm; however, no discernible temperature dependent asymmetries were detected. A laser induced fluorescence signal originating from some impurity has been observed during the course of these experiments on aqueous HAN. This impurity has a broad, structureless, visible absorption spectrum and tests are negative for being of microbe origin.

20. DISTRIBUTION/AVAILABILITY OF ABSTRACT	21. ABSTRACT SECURITY CLASSIFICATION
[X] UNCLASSIFIED/UNLIMITED [ ] SAME AS RPT [ ] DTIC USERS	Unclassified

22a. NAME OF RESPONSIBLE INDIVIDUAL	22b. TELEPHONE (Include Area Code)	22c. OFFICE SYMBOL
MR. STEVEN W. BUNTE	301-278-7068	SLCBR-IB-I

DD FORM 1473, 84 MAR
83 APR edition may be used until exhausted
All other editions are obsolete

SECURITY CLASSIFICATION OF THIS PAGE
UNCLASSIFIED

TABLE OF CONTENTS

LIST OF FIGURES

I. INTRODUCTION

Candidate liquid propellants are composed of aqueous nitrate salts, the major ingredient being hydroxylammonium nitrate. The high solubility of these salts in water allows production of a liquid with sufficient energy content for use as a propellant. Moreover these concentrated salts remain a stable liquid over environmental temperatures exceeding -50 to +50°C.

Macroscopic transport properties such as viscosity and conductivity are of importance in the engineering design of a liquid propellant gun system. Since present theories cannot predict the behavior of these concentrated salt solutions, the properties must be directly measured. In the interest of advancing the understanding of the structure of solutions of HAN, as well as providing a data base, we have been performing Raman spectral measurements on HAN as a function of solute concentration. In an earlier BRL report[1] the experimental technique and some Raman spectra of aqueous HAN were presented. The HA^+ cation, NO_3^- anion and H_2O solvent species were all uniquely identified from their characteristic spectral signatures. This continuing study focuses on the vibrational modes of NO_3^- which have proven extremely useful as a spectroscopic probe of the solution structure. The interactions of the nitrate ion with its surroundings can slightly alter the normal mode vibrational frequencies and is, thus, a sensitive indicator of structural change. Correct interpretations of these vibrational variations can provide information about macroscopic phenomena.

The nitrate ion has six normal modes of vibration, five of which are Raman active; two of these are degenerate. The ν_4 (E') degenerate mode and the ν_1 (A') symmetric stretch mode were more closely investigated to determine changes in vibrational frequencies as a function of concentration. Much of this study was performed to determine whether a case could be made for ion-pairing by analogy with published Raman spectra of other aqueous salts.

Many combinations of ions and solvent molecules with a net charge equal to zero can be envisioned, but the two simplest and most discussed forms are the contact-ion-pair and the solvent-separated-ion-pair. In the strict sense the difference between an undissociated molecule and an ion-pair is that the molecule consists of a number of atoms held together by covalent electronic bonds, whereas the ion-pair is held together entirely by electrostatic Coulomb forces and neither cation nor anion lose their identity. This definition works well for an alkali metal-halide salt. However, when applying the definition to salts such as aqueous HAN where the cation, anion, and solvent molecule can all form hydrogen bonds, the forces involved in ion-pairing can be much more complex.

In 1926, Bjerrum[2] defined the concept of an ion-pair in terms of an interionic distance at which the electrostatic binding energy equals 2kT. That is,

$$b = \frac{|z_1 z_2| e^2}{2\varepsilon kT} ,$$

where a cation and anion which are separated by a distance $\leq b$ are considered paired and longer separations considered free. Z_1 and Z_2 are the valences of

the cation and anion, e is the electrostatic charge, ϵ is the dielectric constant, k is the Boltzmann constant, and T is the absolute temperature. This is certainly a simplified approximation of ion-pairing for the case at hand; nonetheless, some qualitative trends may be determined. For instance, it is known that the dielectric constant of the solvent governs the magnitude of all electrostatic interactions, and, as will be shown, greatly influences ion-pairing.[3] The Bjerrum equation also indicates that ion-pairing is favored as the temperature is lowered. Frost and James[4] have observed this trend for aqueous sodium nitrate solutions, and we have made some measurements on aqueous HAN which is consistent with this trend. It is also well known experimentally that multivalent ions are more apt to ion-pair, but our discussions here will concern only monovalent ions.

II. EXPERIMENTAL

The experimental setup is essentially the same as that discussed in Ref. 1, with a few minor alterations. For the data presented here, the 514.5 nm line of an Ar^+ laser was the source of excitation. Moderate resolution Raman spectra (6 cm^{-1} FWHM) were obtained with a 1/4 m spectrograph-intensified reticon array combination. The spectrograph has a 100 micron entrance slit and a 2400 groove/mm grating. The detector in this configuration could observe about 20 nm of Raman spectra simultaneously. Data from the detector were accumulated by a computer for storage and analysis.

Nominal 13 M aqueous HAN solutions were obtained from Klein of the BRL (dilute aqueous HAN solutions were produced via electrolysis of nitric acid by Southwest Analytical Chemicals, Inc., and then concentrated by solvent stripping under vacuum) and diluted with distilled water to produce some of the less concentrated solutions used in this study. Solid HAN samples were prepared by removing the water from 13 M HAN under vacuum at room temperature. The solid formed was quickly transferred to a spectrophotometer cell and sealed with a rubber finger. At this point the solid had rough irregular surfaces. The sample in the cell was then gently warmed until it liquified. After the sample cooled back to room temperature, it resolidified with a smooth surface usable for spectroscopic studies.

III. RESULTS AND DISCUSSION

Raman spectra of the ν_1 (A_1') symmetric stretch mode of NO_3^- occurring in 3.0, 7.0, 11, 13, and 15 M aqueous HAN solutions are shown in Figure 1. The spectral region displayed is about 900 to 1200 cm^{-1} Stokes shifted from the laser excitation line. Both the ν_1 (A_1') peak at 1048 cm^{-1} and a N-OH vibration at 1010 cm^{-1} can be observed in this region. Some of the characteristics of the spectra are listed in Table 1. On this scale, both peaks in Figure 1 appear symmetric for all the concentrations studied. The ν_1 (A_1') peak position shifts to slightly higher frequencies as the HAN concentration is increased and the linewidth of this transition increases with increasing concentration. This finite linewidth, aside from the instrument function, physically corresponds to a situation where all the anions (NO_3^-) in solution do not have exactly the same environment giving rise to a vibrational frequency distribution around a mean frequency value. This environment can also change with time giving a fluctuating vibrational frequency. The environment surrounding the NO_3^- changes from about eight water molecules per

ion at 3 M to about 0.3 water molecules per ion at 15 M. This change from largely ion-water interactions to anion-cation interactions is responsible for the frequency shift and broadening of the linewidth. Because of these changes in position and linewidth the "apparent" symmetric shape of the ν_1 (A_1') Raman mode could be the result of several symmetric peaks of slightly different mean frequency values where the amplitude of these peaks change as the environment around the NO_3^- changes. Various cation-anion pairing entities have been assigned to deconvolutions of the Raman modes of NO_3^-.

Table 1. Spectral Characteristics of the ν_1 (A_1') and ν_4 (E') NO_3^- Vibrational Modes as a Function of Concentration for Aqueous HAN Solutions

Concentration Molar	ν_1 (A_1') Peak Position cm^{-1}	ν_1 (A_1') Linewidth (FWHM)* cm^{-1}	ν_1 (A_1') Integrated Intensity Arb.	ν_4 (E') Peak Position cm^{-1}	ν_4 (E') Linewidth (FWHM)* cm^{-1}	ν_4 (E') Integrated Intensity Arb.
3	1046.8	8.2	1.14	721.7	18.0	0.87
7	1047.1	9.5	2.63	723.3	19.0	2.17
11	1047.7	10.6	4.14	724.1	19.6	3.56
13	1048.0	11.0	4.87	725.0	20.3	4.25
15	1048.3	12.0	5.69	725.0	+	+
SOLID HAN	1047	<5	----	727.5	<11	

*The spectral resolution is given as full width at half maximum.
+A large fluorescence signal obscured these results.

Using published results as an analogy, some conclusions about aqueous HAN can be drawn. Literature data on spectral characteristics of some monovalent aqueous salts, together with this work for aqueous HAN, are contained in Table 2. It can be seen that all the alkali metal solutions listed[4,5,6] exhibit an increase in Raman frequency and linewidth with increasing concentration. This is true to a lesser extent with K^+, but the saturation limits of K^+ in water prevented a proper comparison at higher concentration. From Table 2 it is seen that NH_3OH^+ exhibits behavior similar to the alkali metal cations and not NH_4^+. One might first think that NH_4^+ is more like NH_3OH^+ since both cations have the ability to form hydrogen bonds. However, Vollmar[5] concluded from his studies that there is similar hydrogen bonding between NO_3^- and either NH_4^+ or H_2O and thus, the environment, as seen by NO_3^-, is not changing as the solute concentration changes.

Many structures have been postulated from curve resolving the ν_1 (A_1') mode of NO_3^-. For aqueous salt solutions, such as $NaNO_3$, which exhibit frequency and linewidth changes with changing concentration Frost and James[4] have resolved the curves into four principal components. These are: a free aquated NO_3^- at 1048 cm^{-1}, a solvent-separated-ion-pair at 1050 cm^{-1}, a contact-ion-pair at 1052 cm^{-1} and larger ion aggregates at 1070 cm^{-1}. By expanding the frequency scale for the ν_1 (A_1') mode as shown in Figure 2, the peak frequency and linewidth differences between 3 and 13 M HAN solutions can

clearly be observed. A least squares procedure was used as an attempt to fit the 13 M curve with two symmetric curves, however, this did not provide any improvement over a single symmetric curve fit. It is still possible that the 13 M curve may be a sum of components, but the resolution of the data does not seem to warrant that type of analysis at this point.

Table 2. Comparison of the Spectral Characteristics of the ν_1 (A_1') Mode of NO_3^- in Aqueous HAN With Published Results for Some Other Aqueous Monovalent Salt Solutions

Cation	Concentration Molar	ν_1 (A_1') Peak Position cm^{-1}	ν_1 (A_1') Linewidth cm^{-1}	References
Li^+	0.85	1048.45	11.68	6
	8.51	1052.07	14.77	6
	0.40		14.8	7
	10.0		18.1	7
	1.0	1048.2	Increases by ~70% over	
	10.0	1051.9	this range	4
Na^+	0.70	1048.9	11.60	6
	7.04	1052.07	13.15	6
	0.56		15.0	7
	7.00		15.8	7
	1.0	1048.4	Increased by ~40% over	
	8.0	1051.1	this range	4
K^+	0.26	1048.41	11.52	6
	2.58	1049.22	11.60	6
	0.5	1048.2	Increases by ~4% over	
	2.75	1049.1	this range	4
NH_4^+	1.00	1048.0	11.56	6
	9.98	1048.0	11.68	6
	1.00	1047.6	Essentially constant over	
	10.00	1047.8	this range	4
NH_3OH^+	3.0	1046.8	8.2	This Work
	11	1047.7	10.6	This Work
	15	1048.3	12.0	This Work

In much more dilute aqueous HAN solutions (about 140 water molecules per ion), it is found that solvation is preferred over ion-pairing. This result follows from analogy with the data of Janz.[3] He demonstrated this behavior with $AgNO_3$ dissolved in various mixtures of water and acetonitrile. With $AgNO_3$ dissolved in water, the ν_1 (A_1') band of NO_3^- exhibits one symmetric peak at ~1046 cm^{-1}. When $AgNO_3$ is dissolved in acetonitrile the ν_1 (A_1') band becomes quite asymmetric and can be resolved into two symmetric peaks centered at 1041 and 1038 cm^{-1}. Dissolving $AgNO_3$ into various mixtures of these solvents cause the relative proportions of these peaks to change. Janz assigns the 1041 cm^{-1} peak to aquated or free NO_3^- and the 1038 cm^{-1} peak to

contact-ion-pairs. In this work, we obtained the Raman spectrum of $AgNO_3$ dissolved in CH_3CN and compared it with the spectra of HAN dissolved in H_2O and then CH_3CN. Figure 3 contains a comparison among: (a) ~0.2 M aqueous HAN, (b) ~0.2 M $AgNO_3$ dissolved in CH_3CN, and (c) ~0.2 M HAN dissolved in CH_3CN. From Table 1 the ν_1 (A_1') mode of NO_3^- is found to occur at 1046.8 cm^{-1} for 3 M aqueous HAN. Using this frequency for 0.2 M aqueous HAN, values of 1036.5 and 1039.8 cm^{-1} are estimated for the double peaked band of Figure 3b. When HAN is dissolved in CH_3CN, the ν_1 (A_1') band shifts to about the same position as $AgNO_3$ in CH_3CN. The shapes of the bands, Figures 3b and 3c, are different, but both are distinctly asymmetric indicating multiple NO_3^- entities. No ion-pairing behavior is exhibited for HAN or $AgNO_3$ with a H_2O solvent. Consequently, we conclude that aquated ions are favored over ion-pairs with the highly polar water solvent which is in accord with Bjerrum's criteria. Nevertheless, the concentrations of interest, around 11 M for propellant applications, are such that there are insufficient water molecules for complete aquation.

Before leaving the symmetric stretch vibration of NO_3^-, a contrast between 13 M aqueous HAN and solid HAN is made in Figure 4. Immediately apparent is the narrowing of the linewidth of the solid HAN vibrational modes. The linewidth decreases from 11 cm^{-1} to values less than 5 cm^{-1} when HAN solidifies. An apparent shift to lower frequencies also occurs upon solidification, see Table 1. Only approximate values for the solid data are given because they appeared time dependent. Experimental spectra were gathered on solid HAN over three consecutive days, and the linewidth was observed to narrow with time. Linewidths typically narrow substantially when changing from liquid to solid phase as the orientational dynamics are frozen out. This decrease in linewidth with time is speculated to be the solid changing from an amorphous to crystalline state. The laser excitation source provides some heating of the sample which could promote this process. More will be said about the solid in the discussion of the ν_4 (E') mode of NO_3^-.

The degenerate in-plane bending mode of NO_3^- has also been investigated for various concentrations and temperatures; these results are displayed in Figures 5 and 6, and Table 1. This ν_4 (E') mode is Raman active only, and extensively referred to in the literature as a diagnostic[7] for the determination of contact-ion-pairing. Unfortunately, the data reported are of only fair-quality for the following reason. The ν_4 (E') mode is about a factor of ten weaker than the ν_1 (A_1') mode which in itself does not cause difficulty. However a laser induced fluorescence impurity signal (to be discussed in more detail later) comprising about 50% of the total ν_4 (E') signal caused the signal-to-noise ratio for this Raman mode to be poor. Nonetheless, we can still distinctly see (Table 1) that both the linewidth and peak position increase with increasing HAN concentration, similar to the behavior of the ν_1 (A_1') mode. With this quality of data, small asymmetries, indicative of any contact-ion-pairing, cannot be unambiguously determined. The type of behavior reported in the literature[7,8] for the ν_4 (E') band of NO_3^- is that a band around 717 cm^{-1} occurs for either aquated NO_3^- or solvent-separated-ion-pairs and another band around 740 cm^{-1} is reported to occur for contact-ion-pairing. Several Raman spectra for the ν_4 (E') mode in 13 M aqueous HAN, see Figure 6, have been obtained over a temperature range from -50 to 22°C. The curve peaking at 725 cm^{-1} is for room temperature (22°C) and this mode shifts to higher frequency as the temperature is decreased. An increase of 4.4 cm^{-1} is observed for a temperature decrease of 72°C. The

-50°C curve appears somewhat asymmetric, however, it was felt that the data is not sufficiently precise to attempt a deconvolution. It is interesting to note that Bjerrum's contact-ion-pairing distance criteria increases with decreasing temperature, and the center frequency of the ν_4 (E') mode moves in the direction of the reported contact-ion-pair frequency as the temperature is decreased. Our results for this Raman mode are consistent with the presence of aquated ions, solvent-separated-ion-pairs, and a small amount of contact ion-pairing existing in the concentration range studied.

Dramatic time dependent changes were observed to occur in the ν_4 (E') Raman mode for the solid HAN that we produced. A Raman spectrum of 13 M HAN is contrasted with three spectra of solid HAN taken on three consecutive days after preparation, see Figure 7. Here again the linewidth decreases upon solidification, however, the frequency increases upon solidification contrary to the behavior of the ν_1 (A_1') mode. From day 1 to 3 the linewidth decreased and two or more bands appeared with center frequencies around 724 and 730 cm^{-1}. Fifer's[9] Fourier transform infrared studies of solid HAN also show two NO_3^- bands appearing at the same frequencies. Again the explanation offered for the time dependence is changing from an amorphous to a crystalline state.

As a consistency check on the experimental data for the ν_1 (A_1') and ν_4 (E') Raman bands, their integrated intensities were obtained as a function of concentration and the results are shown in Table 1 and plotted in Figure 8. The proper linear behavior is demonstrated and a straight line extrapolation of the ν_1 (A_1') data passes through the origin as required, however, the ν_4 (E') extrapolation does not. Improper subtraction of the laser induced fluorescence impurity background is probably responsible for this variation.

This laser induced fluorescence background was observed to vary substantially for three different lots of aqueous HAN solutions studied, as can be observed in the low resolution Raman spectra of 13 M aqueous HAN shown in Figure 9. The fluorescence contribution, ranging from about 40% (bottom spectra) to over 90% of the total signal, can seriously impair spectroscopic probing. Several other tests have been performed to characterize the nature of this impurity. As seen by eye it is apparent that the degree of yellowing of the solution is proportional to the amount of impurity. Two absorption spectra, Figure 10, are shown for the 13 M aqueous HAN solutions that produced the bottom and top Raman spectra of Figure 9. The large absorption at wavelengths less than 350 nm is due to the nitrate ions, but in addition, there is a substantial broad structureless absorption extending to wavelengths beyond 550 nm, and this absorption must come from impurities. Since the absorption spectrum appeared structureless, tests for possible microbe contamination were performed. Microscope examination and culturing on several media, however, gave negative results. NO_2 has been suggested as a possible decomposition product which could be consistent with these observations. To date, experiments to detect trace amounts of this species have not been attempted. Any substantial amounts of NO_2 should lead to rapid sample decomposition, and this is not observed. The yellowish samples exist for many months without appreciable decomposition.

IV. SUMMARY

From Raman investigations on the nitrate anion existing in aqueous HAN solutions and a comparison with published results for other monovalent aqueous salt solutions, some general structural characteristics of aqueous HAN have been determined. In dilute HAN solutions, solvated ions are favored over contact-ion-pairs. This phenomena is observed, in general, for monovalent salts when the solvent has a large dielectric constant such as water. As the concentration of HAN is increased, complete solvation or aquation is no longer possible. At such concentrations, solvent-separated-ion-pairs and contact-ion-pairs can exist. The entities do not exist in isolation since the concentration of solute is such that there are other ions in the near vicinity. Because of the influence of many ions on each other, the Raman spectral perturbations can be less than for isolated contact-ion-pairs as one would have in systems where the solvent has a low dielectric constant. Lastly, an impurity causing laser induced fluorescence signals has been partially characterized. This impurity is not associated with any appreciable decomposition of the material; nonetheless, it can seriously degrade certain spectroscopic observations.

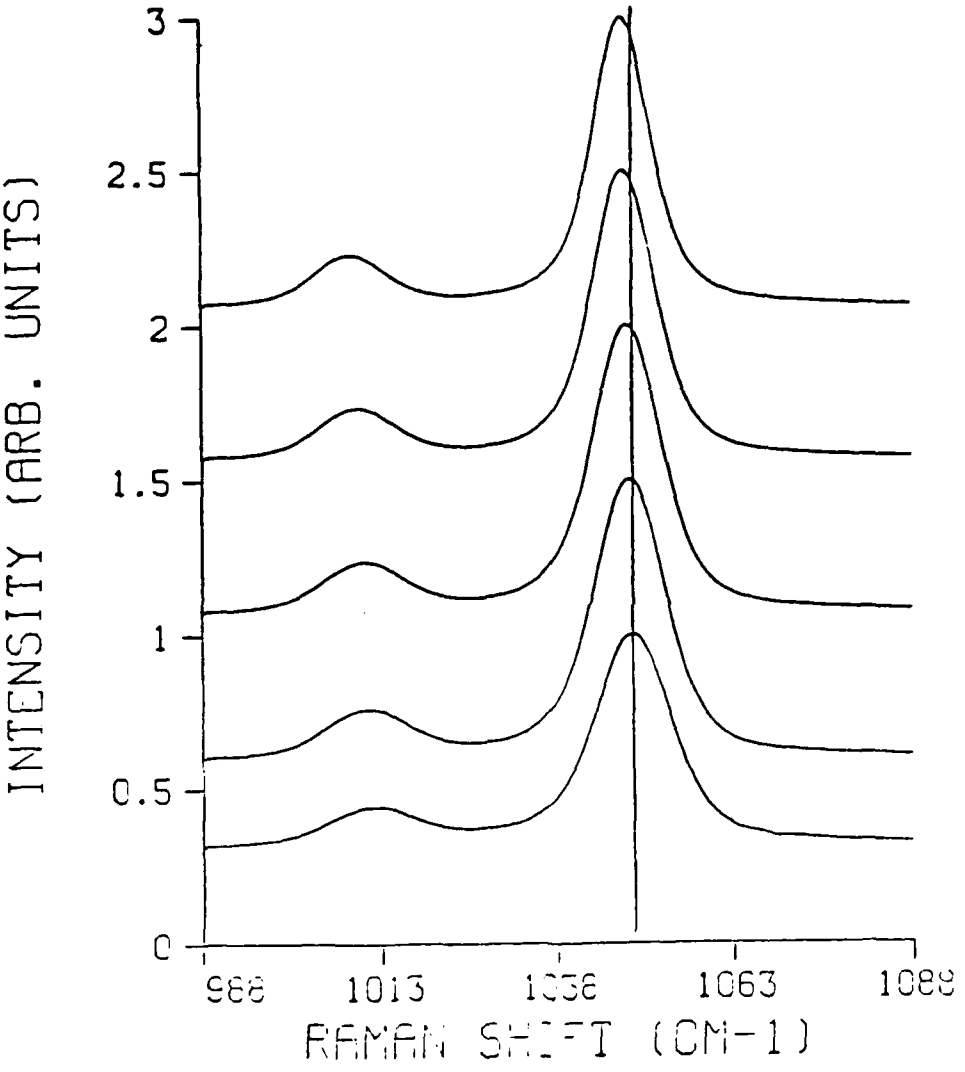

Figure 1. Raman Spectra of the ν_1 (A_1') Mode of NO_3^- Taken for 3, 7, 11, 13, and 15 M Aqueous HAN Solutions. The concentrations are displayed in order; 3 M being the top spectrum. The vertical line is drawn in to emphasize the frequency shift.

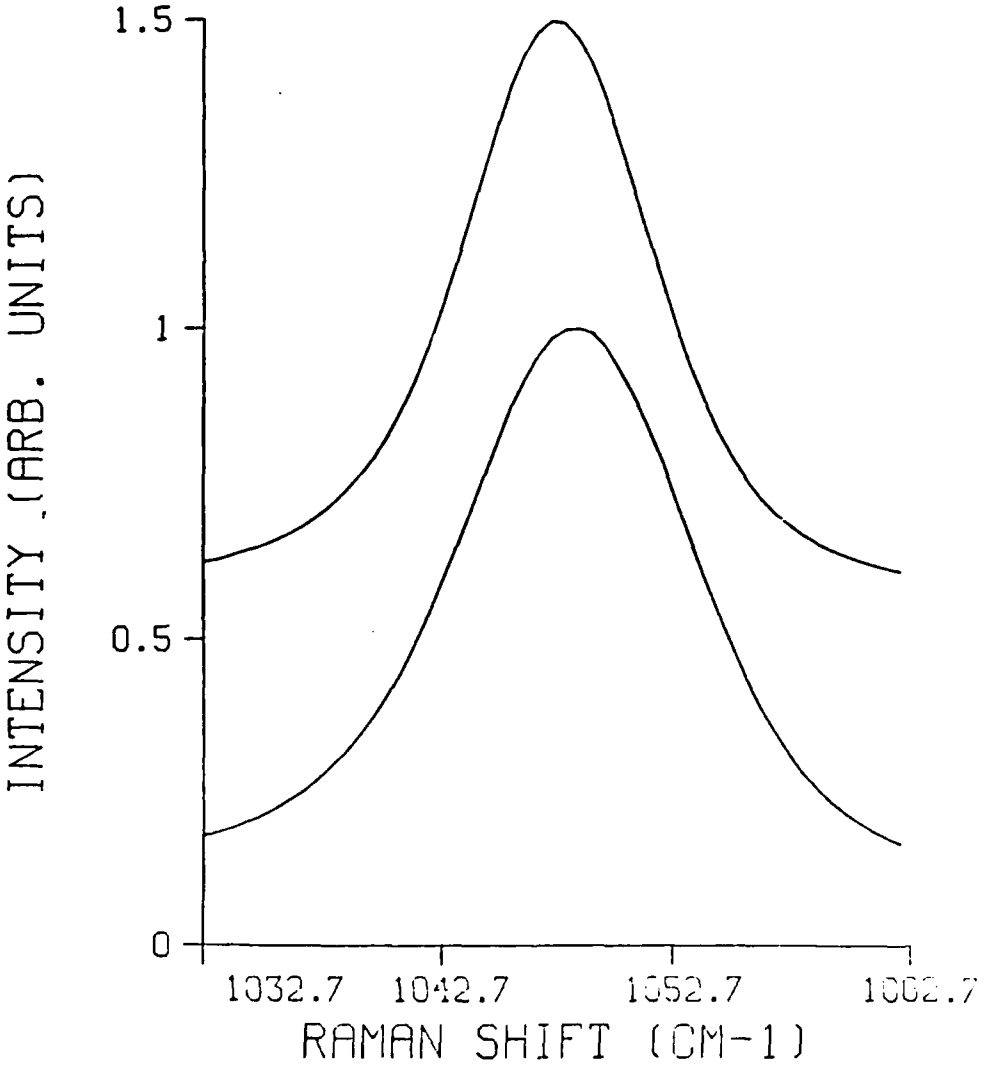

Figure 2. Raman Spectra of the ν_1 (A_1') Mode of NO_3^- Taken for 3 and 13 M Aqueous HAN. The top spectrum is 3 M. The frequency scale has been expanded about threefold from that of Figure 1.

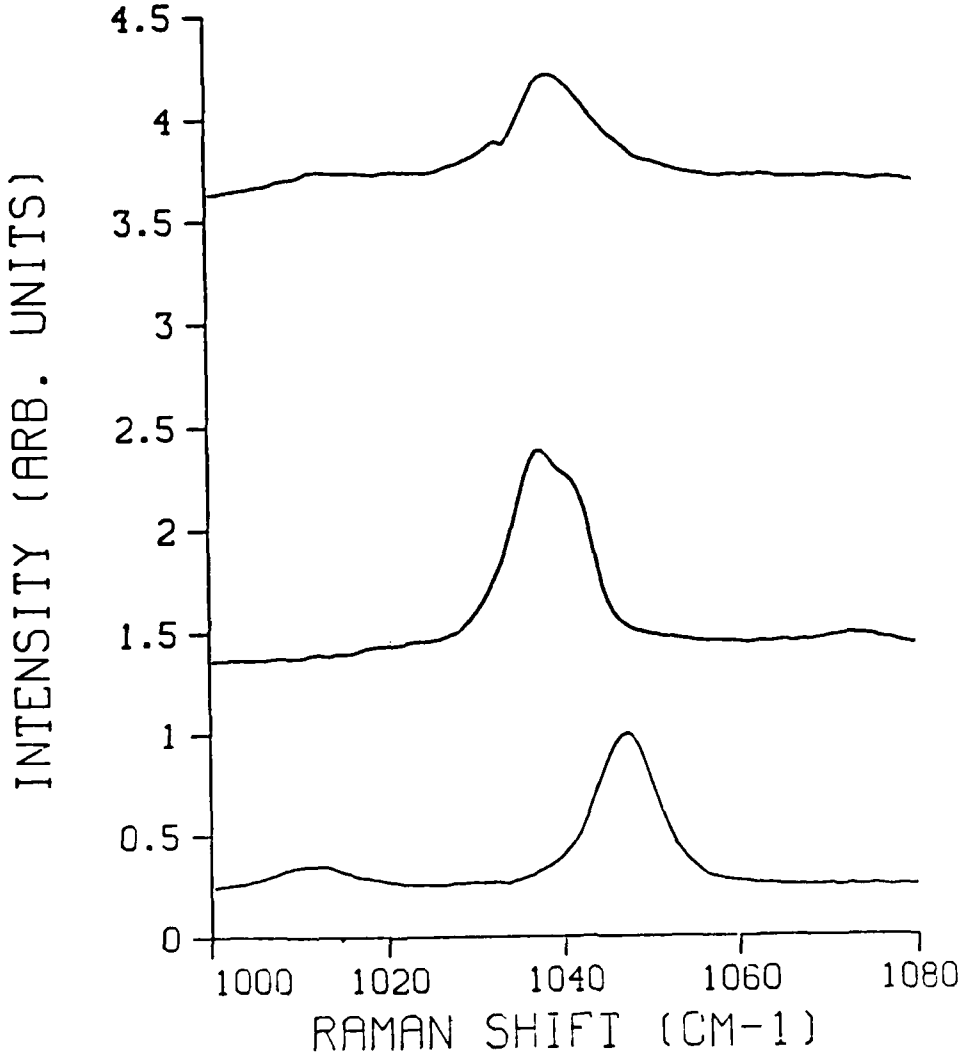

Figure 3. Raman Spectra of the ν_1 (A_1') Mode of NO_3^- Taken for ~0.2 M HAN Dissolved in CH_3CN (Top Spectrum), ~0.2 M $AgNO_3$ Dissolved in CH_3CN (Middle Spectrum), and ~0.2 M Aqueous HAN (Bottom Spectrum)

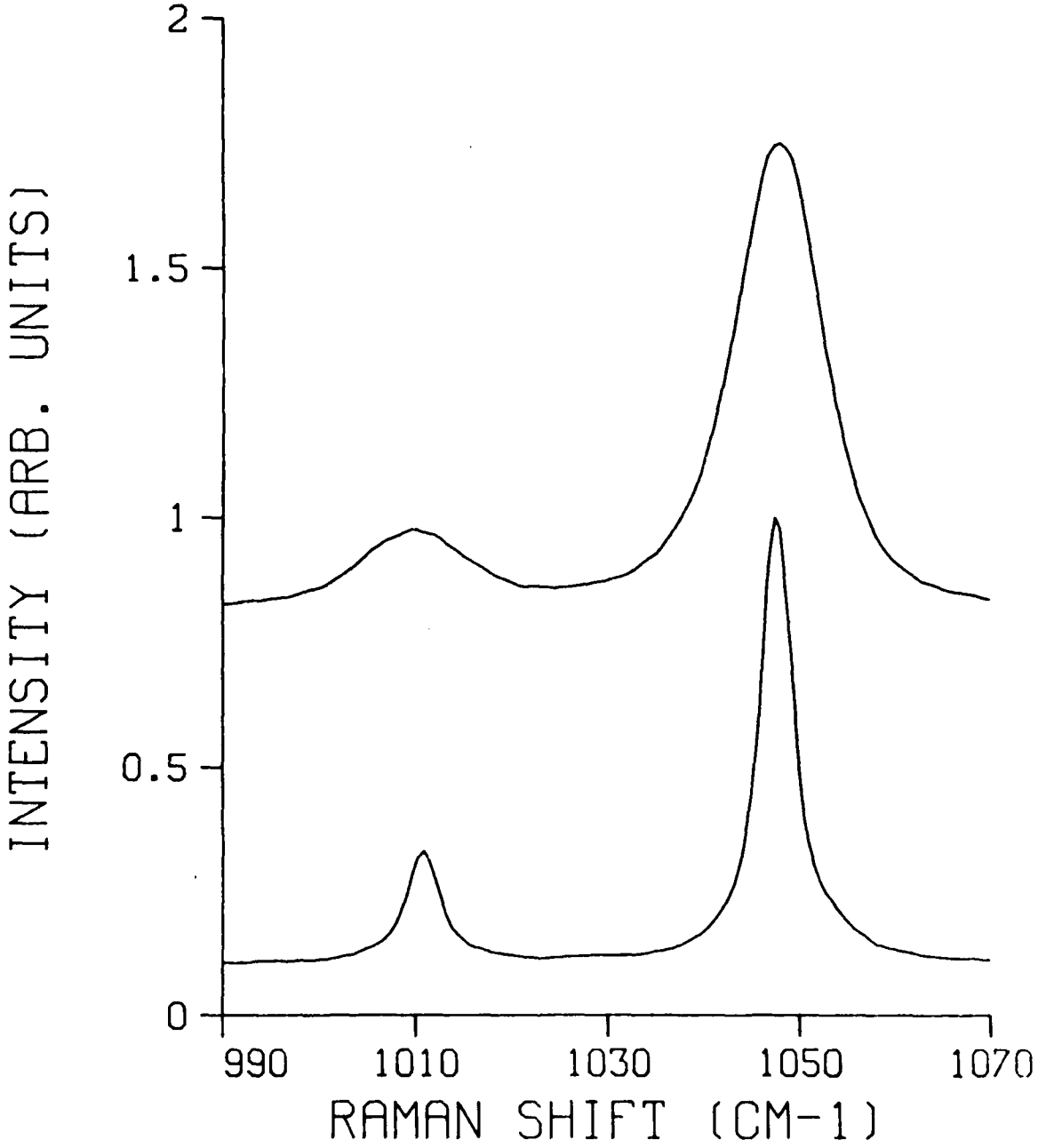

Figure 4. Raman Spectra of the ν_1 (A_1') Mode of NO_3^- Taken for 13 M Aqueous HAN (Top Spectrum) and Solid HAN

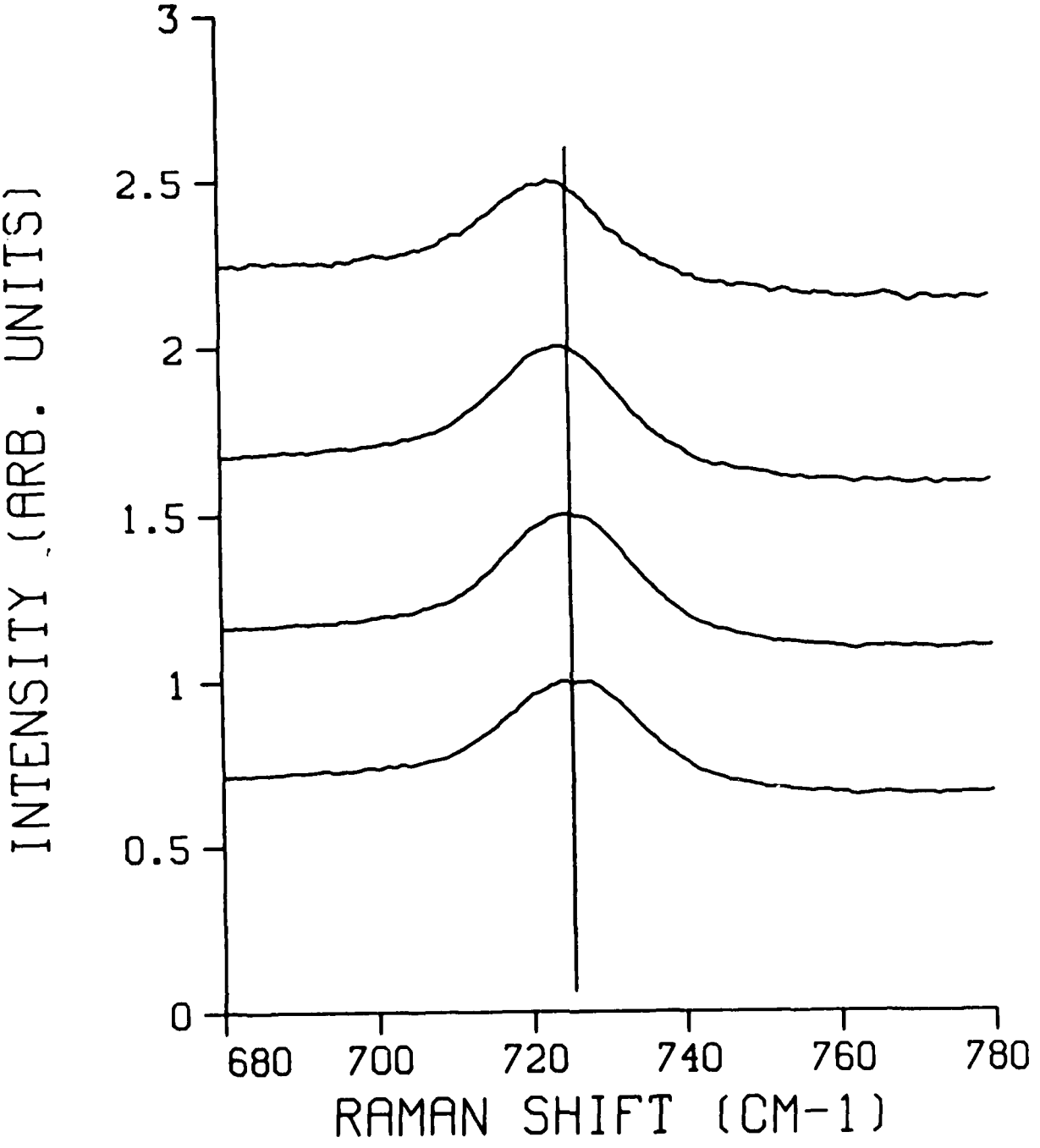

Figure 5. Raman Spectra of the ν_4 (E') Mode of NO_3^- Taken for 3, 7, 11, and 13 M Aqueous HAN Solutions. The concentrations are displayed in order; 3 M being the top spectrum. The vertical line is drawn in to emphasize the frequency shift.

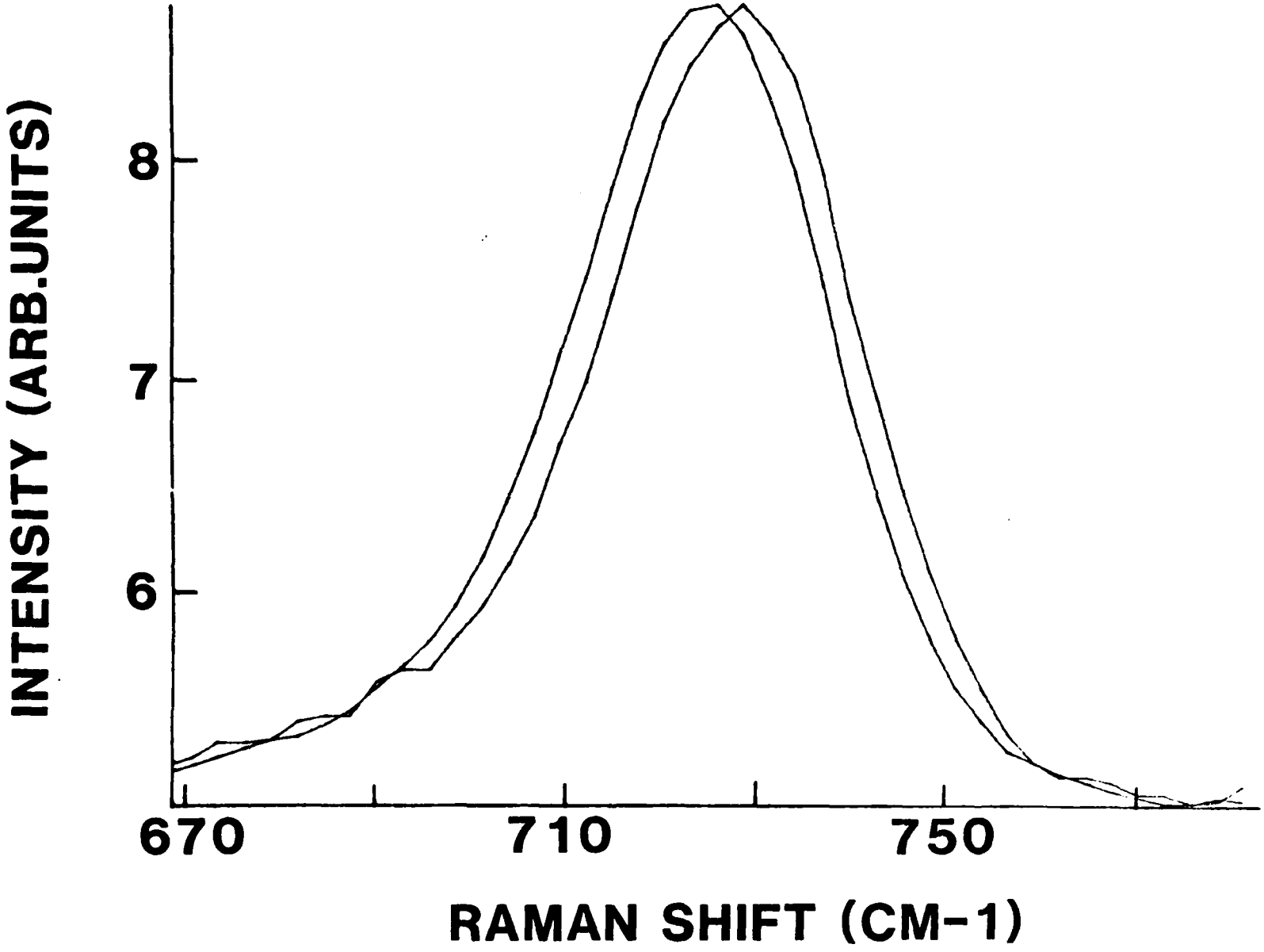

Figure 6. Raman Spectra of the ν_4 (E') Mode of NO_3^- Taken for 13 M Aqueous HAN. The spectrum to the left (lowest frequency peak) is for a temperature of 22°C; the other a temperature of -50°C.

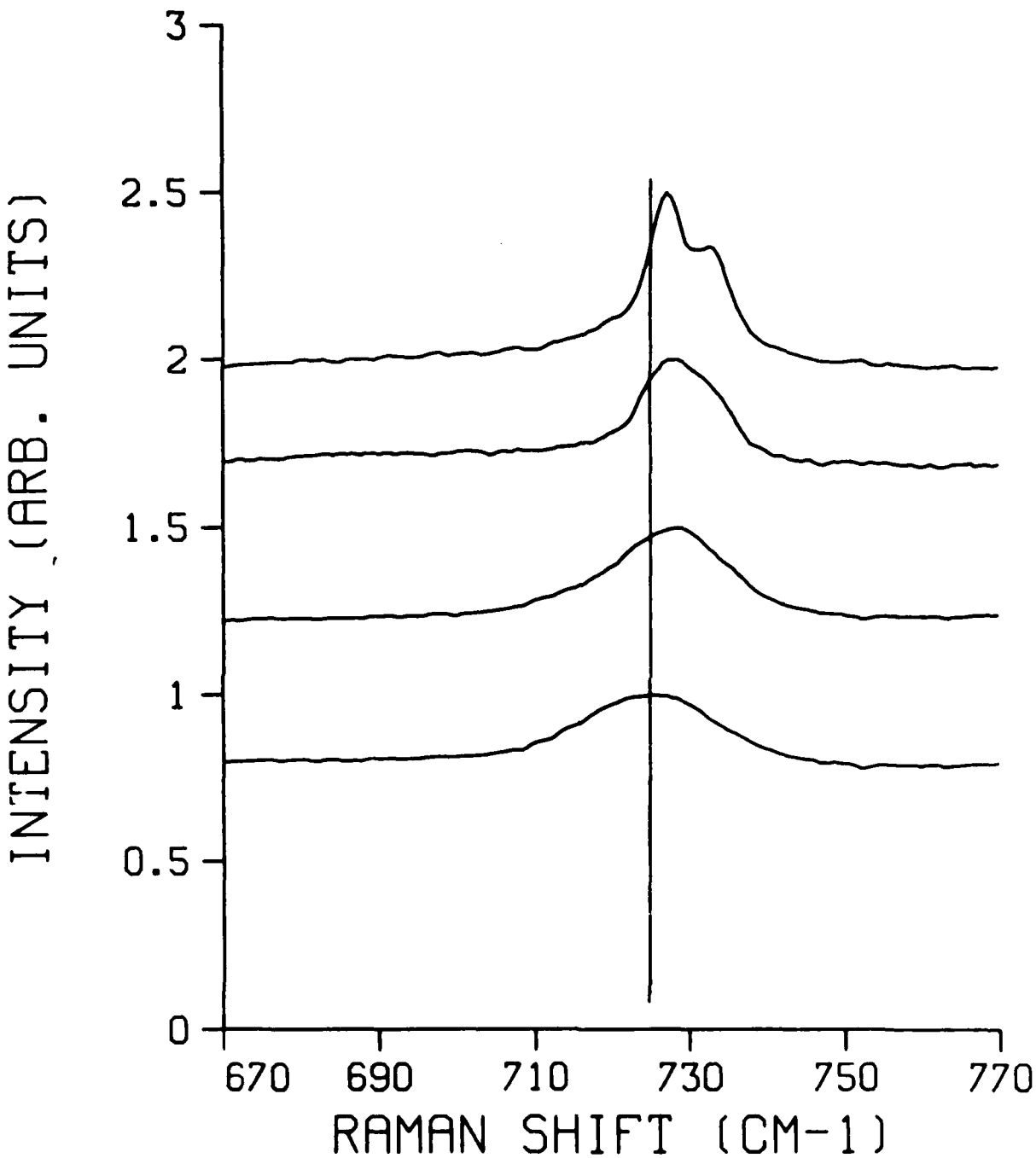

Figure 7. Raman Spectra of the ν_4 (E') Mode of NO_3^- Taken for 13 M Aqueous HAN (Bottom Spectrum), Solid HAN on Day 1 (Next Spectrum), Solid HAN on Day 2 (Next Spectrum), and Solid HAN on Day 3 (Top Spectrum). The vertical line is drawn in to emphasize the frequency shift.

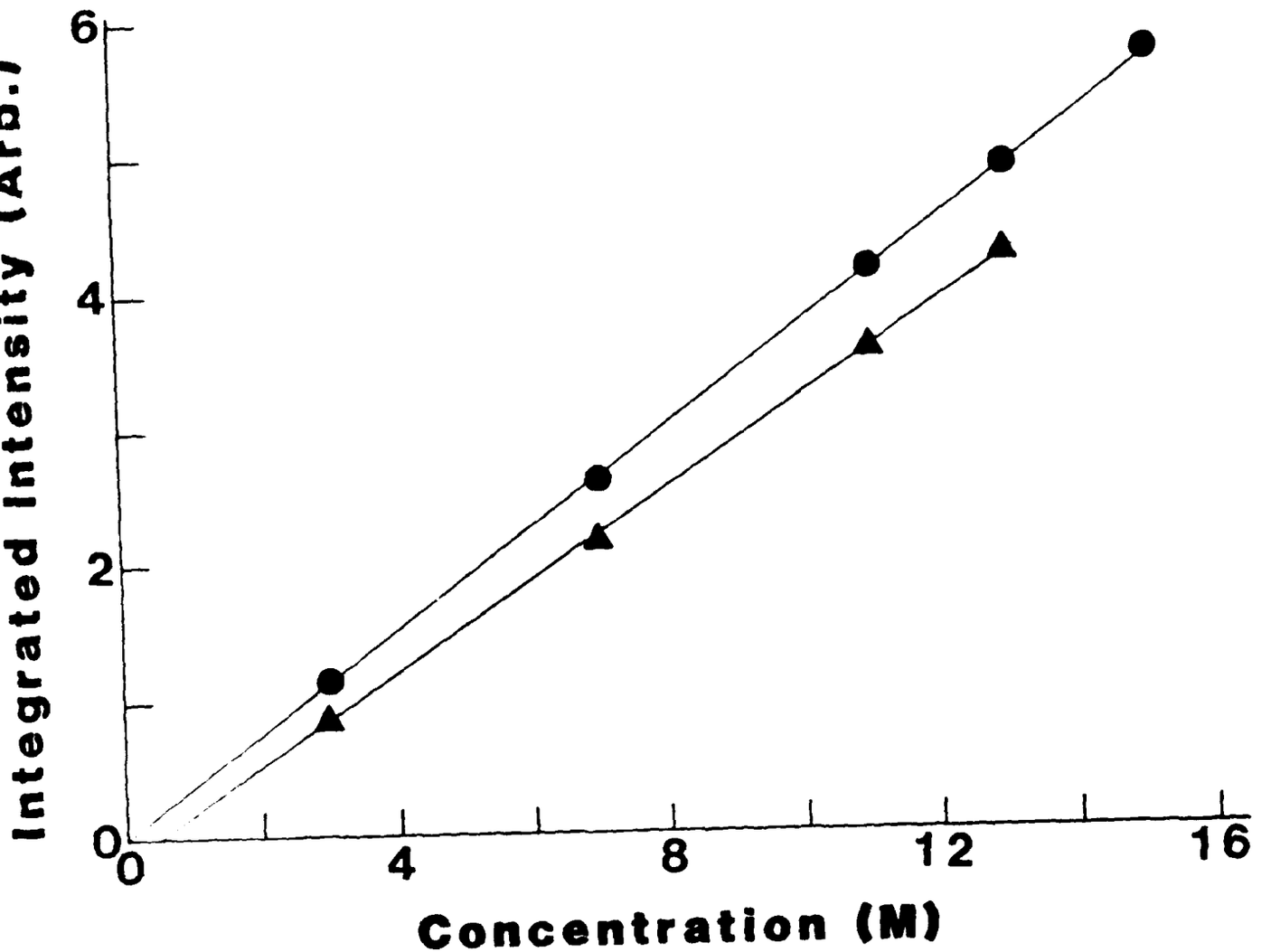

Figure 8. Integrated Intensity of Two NO_3^- Raman Bands in Aqueous HAN Plotted as a Function of Concentration. The circles represent data for the ν_1 (A_1') mode and the triangles are data for the ν_4 (E') mode.

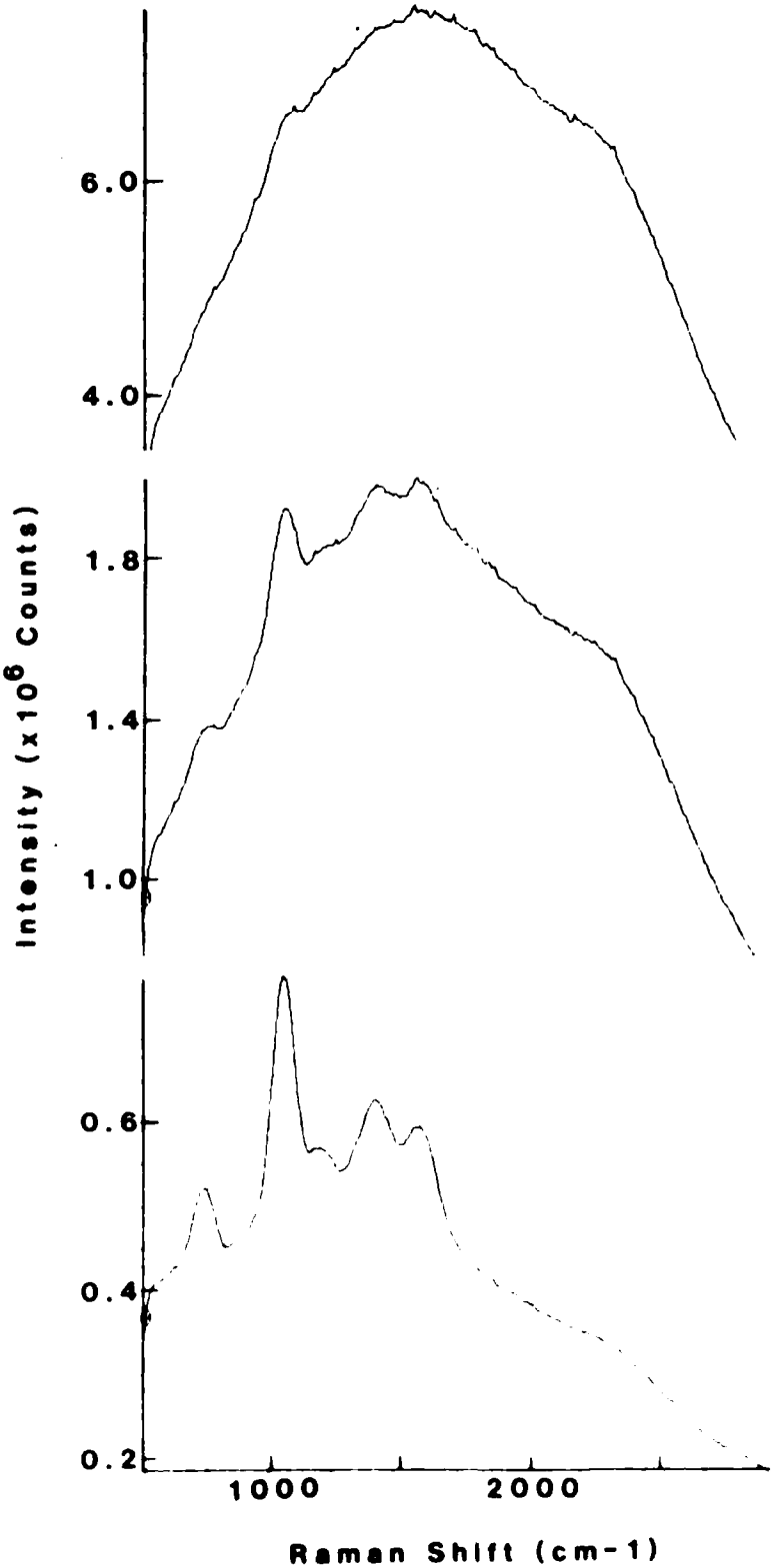

Figure 9. Raman Spectra for 13 M Aqueous HAN Solutions Showing the Effect of a Fluorescence Impurity. Maximum impurity is in the top spectrum, decreasing downward.

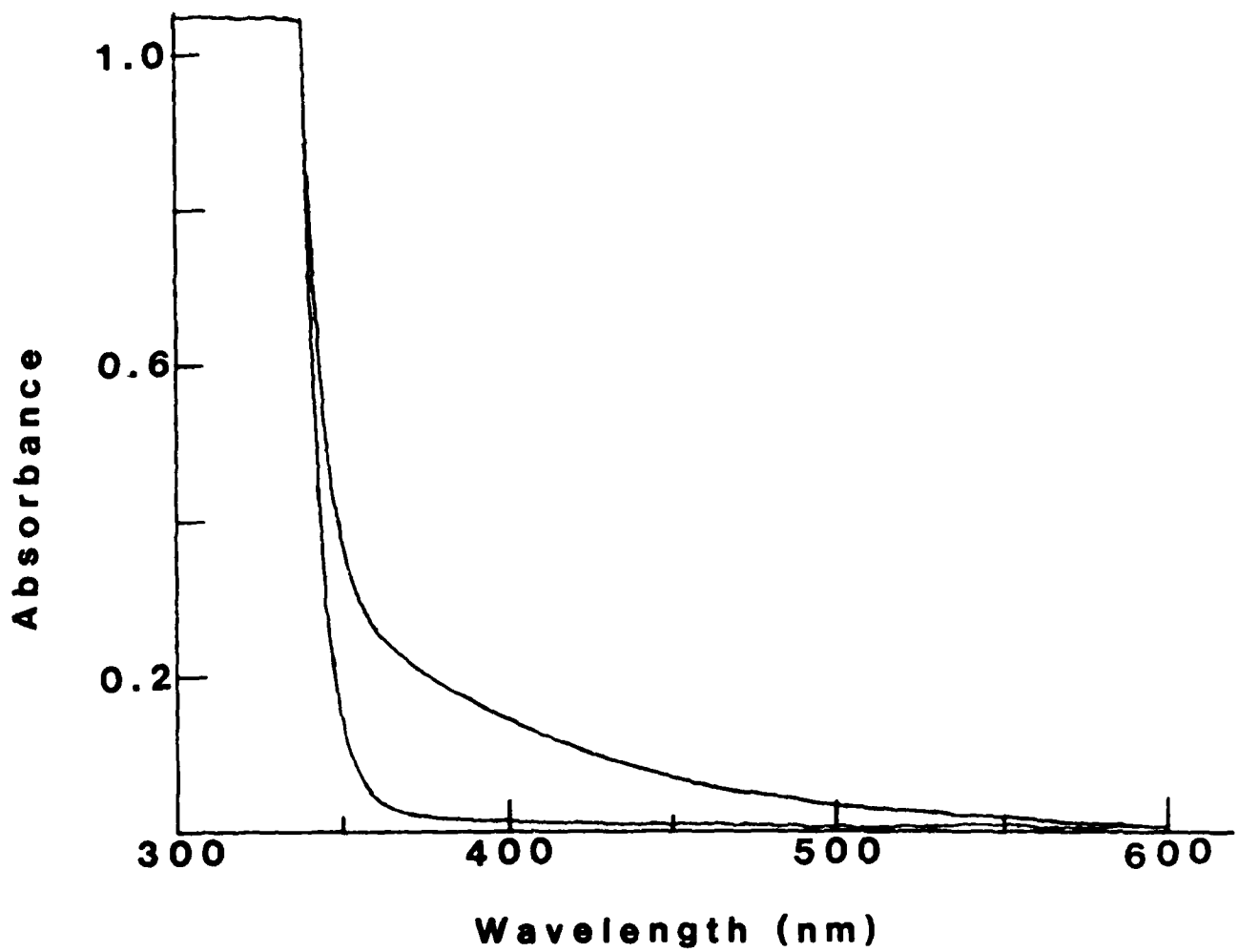

Figure 10. Absorption Spectra for Two 13 M Aqueous HAN Solutions with Differing Amounts of Fluorescence Impurity

REFERENCES

1. J.A. Vanderhoff, S.W. Bunte, and A.W. Miziolek, "Laser Raman Studies Related to Liquid Propellants," BRL-TR-2657, June 1985.

2. N.K. Bjerrum, Danske Vidensk Selsk., Vol. 7, No. 9, p. 1926, "Selected Papers," p. 108, Einar Munksgaard, Copenhagen, 1949.

3. G.J. Janz, "Studies of Ionic Association and Solvation with Raman Laser Spectroscopy," J. Electroanal. Chem., Vol. 29, p. 107, 1971.

4. R.L. Frost and D.W. James, "Ion-Ion-Solvent Interactions in Solution," J. Chem. Soc. Faraday Trans. I, Vol. 78, p. 3223, 1982.

5. P.M. Vollmar, "Ionic Interactions in Aqueous Solution: A Raman Spectral Study", J. Chem. Phys., Vol. 39, p. 2236, 1963.

6. D.E. Irish and A.R. Davis, "Interactions in Aqueous Alkali Metal Nitrate Solutions", Can. J. Chem., Vol. 46, p. 943, 1968.

7. D.E. Irish and M.H. Brooker, "Raman and Infrared Studies of Electrolytes", in Advances in Infrared and Raman Spectroscopy, Vol. II, R.J.H. Clark and R.E. Hester, eds., Heyden & Son, Ltd., New York, NY, 1976.

8. D.E. Irish, D.L. Nelson, and M.H. Brooker, "Quasi-Lattice Features of Concentrated Aqueous $LiNO_3$ Solutions", J. Chem. Phys., Vol. 54, p. 654, 1971.

9. R.A. Fifer, private communication.

DISTRIBUTION LIST

No. Of Copies	Organization
12	Administrator Defense Technical Info Center ATTN: DTIC-FDAC Cameron Station, Bldg. 5 Alexandria, VA 22304-6145
1	HQ DA DAMA-ART-M Washington, DC 20310
1	Commander US Army Materiel Command ATTN: AMCDRA-ST 5001 Eisenhower Avenue Alexandria, VA 22333-0001
10	C.I.A. OIR/DB/Standard GE47 HQ Washington, DC 20505
1	Commander US Army ARDEC ATTN: SMCAR-MSI Dover, NJ 07801-5001
1	Commander US Army ARDEC ATTN: SMCAR-TDC Dover, NJ 07801
1	Commander US AMCCOM ARDEC CCAC Benet Weapons Laboratory ATTN: SMCAR-CCB-TL Watervliet, NY 12189-4050
1	US Army Armament, Munitions and Chemical Command ATTN: AMSMC-IMP-L Rock Island, IL 61299-7300
1	Commander US Army Aviation Systems Command ATTN: AMSAV-ES 4300 Goodfellow Blvd. St. Louis, MO 63120-1798
1	Director US Army Aviation Research and Technology Activity Ames Research Center Moffett Field, CA 94035-1099
4	Commander US Army Research Office ATTN: R. Ghirardelli D. Mann R. Singleton R. Shaw P.O. Box 12211 Research Triangle Park, NC 27709-2211
1	Commander US Army Communications - Electronics Command ATTN: AMSEL-ED Fort Monmouth, NJ 07703
1	Commander CECOM R&D Technical Library ATTN: AMSEL-IM-L, Reports Section B.2700 Fort Monmouth, NJ 07703-5000
2	Commander Armament R&D Center US Army AMCCOM ATTN: SMCAR-LCA-G, D.S. Downs J.A. Lannon Dover, NJ 07801
1	Commander Armament R&D Center US Army AMCCOM ATTN: SMCAR-LC-G, L. Harris Dover, NJ 07801
1	Commander Armament R&D Center US Army AMCCOM ATTN: SMCAR-SCA-T, L. Stiefel Dover, NJ 07801

DISTRIBUTION LIST

No. Of Copies	Organization
1	Commander US Army Missile Command Research, Development and Engineering Center ATTN: AMSMI-RD Redstone Arsenal, AL 35898
1	Commander US Army Missile and Space Intelligence Center ATTN: AMSMI-YDL Redstone Arsenal, AL 35898-5000
2	Commander US Army Missile Command ATTN: AMSMI-RK, D.J. Ifshin W. Wharton Redstone Arsenal, AL 35898
1	Commander US Army Missile Command ATTN: AMSMI-RKA, A.R. Maykut Redstone Arsenal, AL 35898-5249
1	Commander US Army Tank Automotive Command ATTN: AMSTA-TSL Warren, MI 48397-5000
1	Director US Army TRADOC Systems Analysis Center ATTN: ATOR-TSL White Sands Missile Range, NM 88002-5502
1	Commandant US Army Infantry School ATTN: ATSH-CD-CS-OR Fort Benning, GA 31905-5400
1	Commander US Army Development and Employment Agency ATTN: MODE-ORO Fort Lewis, WA 98433-5000

No. Of Copies	Organization
1	Office of Naval Research Department of the Navy ATTN: R.S. Miller, Code 432 800 N. Quincy Street Arlington, VA 22217
1	Commander Naval Air Systems Command ATTN: J. Ramnarace, AIR-54111C Washington, DC 20360
2	Commander Naval Ordnance Station ATTN: C. Irish P.L. Stang, Code 515 Indian Head, MD 20640
1	Commander Naval Surface Weapons Center ATTN: J.L. East, Jr., G-23 Dahlgren, VA 22448-5000
2	Commander Naval Surface Weapons Center ATTN: R. Bernecker, R-13 G.B. Wilmot, R-16 Silver Spring, MD 20902-5000
1	Commander Naval Weapons Center ATTN: R.L. Derr, Code 389 China Lake, CA 93555
2	Commander Naval Weapons Center ATTN: Code 3891, T. Boggs K.J. Graham China Lake, CA 93555
5	Commander Naval Research Laboratory ATTN: M.C. Lin J. McDonald E. Oran J. Shnur R.J. Doyle, Code 6110 Washington, DC 20375

DISTRIBUTION LIST

No. Of Copies	Organization
1	Commanding Officer Naval Underwater Systems Center Weapons Dept. ATTN: R.S. Lazar/Code 36301 Newport, RI 02840
1	Superintendent Naval Postgraduate School Dept. of Aeronautics ATTN: D.W. Netzer Monterey, CA 93940
4	AFRPL/DY, Stop 24 ATTN: R. Corley R. Geisler J. Levine D. Weaver Edwards AFB, CA 93523-5000
1	AFRPL/MKPB, Stop 24 ATTN: B. Goshgarian Edwards AFB, CA 93523-5000
1	AFOSR ATTN: J.M. Tishkoff Bolling Air Force Base Washington, DC 20332
1	AFATL/DOIL (Tech Info Center) Eglin AFB, FL 32542-5438
1	Air Force Weapons Laboratory AFWL/SUL ATTN: V. King Kirtland AFB, NM 87117
1	NASA Langley Research Center Langley Station ATTN: G.B. Northam/MS 168 Hampton, VA 23365
4	National Bureau of Standards ATTN: J. Hastie M. Jacox T. Kashiwagi H. Semerjian US Department of Commerce Washington, DC 20234
1	OSD/SDIO/UST ATTN: L.H. Caveny Pentagon Washington, DC 20301-7100
1	Aerojet Solid Propulsion Co. ATTN: P. Micheli Sacramento, CA 95813
1	Applied Combustion Technology, Inc. ATTN: A.M. Varney P.O. Box 17885 Orlando, FL 32860
2	Applied Mechanics Reviews The American Society of Mechanical Engineers ATTN: R.E. White A.B. Wenzel 345 E. 47th Street New York, NY 10017
1	Atlantic Research Corp. ATTN: M.K. King 5390 Cherokee Avenue Alexandria, VA 22314
1	Atlantic Research Corp. ATTN: R.H.W. Waesche 7511 Wellington Road Gainesville, VA 22065
1	AVCO Everett Rsch. Lab. Div. ATTN: D. Stickler 2385 Revere Beach Parkway Everett, MA 02149
1	Battelle Memorial Institute Tactical Technology Center ATTN: J. Huggins 505 King Avenue Columbus, OH 43201
1	Cohen Professional Services ATTN: N.S. Cohen 141 Channing Street Redlands, CA 92373

DISTRIBUTION LIST

No. Of Copies	Organization
1	Exxon Research & Eng. Co. Government Research Lab ATTN: A. Dean P.O. Box 48 Linden, NJ 07036
1	Ford Aerospace and Communications Corp. DIVAD Division Div. Hq., Irvine ATTN: D. Williams Main Street & Ford Road Newport Beach, CA 92663
1	General Applied Science Laboratories, Inc. ATTN: J.I. Erdos 425 Merrick Avenue Westbury, NY 11590
1	General Electric Armament & Electrical Systems ATTN: M.J. Bulman Lakeside Avenue Burlington, VT 05401
1	General Electric Company 2352 Jade Lane Schenectady, NY 12309
1	General Electric Ordnance Systems ATTN: J. Mandzy 100 Plastics Avenue Pittsfield, MA 01203
2	General Motors Rsch Labs Physics Department ATTN: T. Sloan R. Teets Warren, MI 48090
2	Hercules, Inc. Allegany Ballistics Lab. ATTN: R.R. Miller E.A. Yount P.O. Box 210 Cumberland, MD 21501
1	Hercules, Inc. Bacchus Works ATTN: K.P. McCarty P.O. Box 98 Magna, UT 84044
1	Honeywell, Inc. Government and Aerospace Products ATTN: D.E. Broden/ MS MN50-2000 600 2nd Street NE Hopkins, MN 55343
1	IBM Corporation ATTN: A.C. Tam Research Division 5600 Cottle Road San Jose, CA 95193
1	IIT Research Institute ATTN: R.F. Remaly 10 West 35th Street Chicago, IL 60616
2	Director Lawrence Livermore National Laboratory ATTN: C. Westbrook M. Costantino P.O. Box 808 Livermore, CA 94550
1	Lockheed Missiles & Space Co. ATTN: George Lo 3251 Hanover Street Dept. 52-35/B204/2 Palo Alto, CA 94304
1	Los Alamos National Lab ATTN: B. Nichols T7, MS-B284 P.O. Box 1663 Los Alamos, NM 87545
1	National Science Foundation ATTN: A.B. Harvey Washington, DC 20550

DISTRIBUTION LIST

No. Of Copies	Organization
1	Olin Corporation Smokeless Powder Operations ATTN: V. McDonald P.O. Box 222 St. Marks, FL 32355
1	Paul Gough Associates, Inc. ATTN: P.S. Gough 1048 South Street Portsmouth, NH 03801
2	Princeton Combustion Research Laboratories, Inc. ATTN: M. Summerfield N.A. Messina 475 US Highway One Monmouth Junction, NJ 08852
1	Hughes Aircraft Company ATTN: T.E. Ward 8433 Fallbrook Avenue Canoga Park, CA 91303
1	Rockwell International Corp. Rocketdyne Division ATTN: J.E. Flanagan/HB02 6633 Canoga Avenue Canoga Park, CA 91304
4	Sandia National Laboratories Combustion Sciences Dept. ATTN: R. Cattolica S. Johnston P. Mattern D. Stephenson Livermore, CA 94550
1	Science Applications, Inc. ATTN: R.B. Edelman 23146 Cumorah Crest Woodland Hills, CA 91364
1	Science Applications, Inc. ATTN: H.S. Pergament 1100 State Road, Bldg. N Princeton, NJ 08540
3	SRI International ATTN: G. Smith D. Crosley D. Golden 333 Ravenswood Avenue Menlo Park, CA 94025
1	Stevens Institute of Tech. Davidson Laboratory ATTN: R. McAlevy, III Hoboken, NJ 07030
1	Textron, Inc. Bell Aerospace Co. Division ATTN: T.M. Ferger P.O. Box 1 Buffalo, NY 14240
1	Thiokol Corporation Elkton Division ATTN: W.N. Brundige P.O. Box 241 Elkton, MD 21921
1	Thiokol Corporation Huntsville Division ATTN: R. Glick Huntsville, AL 35807
3	Thiokol Corporation Wasatch Division ATTN: S.J. Bennett P.O. Box 524 Brigham City, UT 84302
1	TRW ATTN: M.S. Chou MSR1-1016 1 Parke Redondo Beach, CA 90278
1	United Technologies ATTN: A.C. Eckbreth East Hartford, CT 06108

DISTRIBUTION LIST

No. Of Copies	Organization
3	United Technologies Corp. Chemical Systems Division ATTN: R.S. Brown T.D. Myers (2 copies) P.O. Box 50015 San Jose, CA 95150-0015
2	United Technologies Corp. ATTN: R.S. Brown R.O. McLaren P.O. Box 358 Sunnyvale, CA 94086
1	Universal Propulsion Company ATTN: H.J. McSpadden Black Canyon Stage 1 Box 1140 Phoenix, AZ 85029
1	Veritay Technology, Inc. ATTN: E.B. Fisher 4845 Millersport Highway P.O. Box 305 East Amherst, NY 14051-0305
1	Brigham Young University Dept. of Chemical Engineering ATTN: M.W. Beckstead Provo, UT 84601
1	California Institute of Tech. Jet Propulsion Laboratory ATTN: MS 125/159 4800 Oak Grove Drive Pasadena, CA 91103
1	California Institute of Technology ATTN: F.E.C. Culick/ MC 301-46 204 Karman Lab. Pasadena, CA 91125
1	University of California, Berkeley Mechanical Engineering Dept. ATTN: J. Daily Berkeley, CA 94720
1	University of California Los Alamos Scientific Lab. P.O. Box 1663, Mail Stop B216 Los Alamos, NM 87545
2	University of California, Santa Barbara Quantum Institute ATTN: K. Schofield M. Steinberg Santa Barbara, CA 93106
2	University of Southern California Dept. of Chemistry ATTN: S. Benson C. Wittig Los Angeles, CA 90007
1	Case Western Reserve Univ. Div. of Aerospace Sciences ATTN: J. Tien Cleveland, OH 44135
1	Cornell University Department of Chemistry ATTN: T.A. Cool Baker Laboratory Ithaca, NY 14853
1	Univ. of Dayton Rsch Inst. ATTN: D. Campbell AFRPL/PAP Stop 24 Edwards AFB, CA 93523
1	University of Florida Dept. of Chemistry ATTN: J. Winefordner Gainesville, FL 32611
3	Georgia Institute of Technology School of Aerospace Engineering ATTN: E. Price W.C. Strahle B.T. Zinn Atlanta, GA 30332

DISTRIBUTION LIST

No. Of Copies	Organization
1	University of Illinois Dept. of Mech. Eng. ATTN: H. Krier 144MEB, 1206 W. Green St. Urbana, IL 61801
1	Johns Hopkins University/APL Chemical Propulsion Information Agency ATTN: T.W. Christian Johns Hopkins Road Laurel, MD 20707
1	University of Michigan Gas Dynamics Lab Aerospace Engineering Bldg. ATTN: G.M. Faeth Ann Arbor, MI 48109-2140
1	University of Minnesota Dept. of Mechanical Engineering ATTN: E. Fletcher Minneapolis, MN 55455
3	Pennsylvania State University Applied Research Laboratory ATTN: K.K. Kuo H. Palmer M. Micci University Park, PA 16802
1	Polytechnic Institute of NY Graduate Center ATTN: S. Lederman Route 110 Farmingdale, NY 11735
2	Princeton University Forrestal Campus Library ATTN: K. Brezinsky I. Glassman P.O. Box 710 Princeton, NJ 08540
1	Princeton University MAE Dept. ATTN: F.A. Williams Princeton, NJ 08544
1	Purdue University School of Aeronautics and Astronautics ATTN: J.R. Osborn Grissom Hall West Lafayette, IN 47906
1	Purdue University Department of Chemistry ATTN: E. Grant West Lafayette, IN 47906
2	Purdue University School of Mechanical Engineering ATTN: N.M. Laurendeau S.N.B. Murthy TSPC Chaffee Hall West Lafayette, IN 47906
1	Rensselaer Polytechnic Inst. Dept. of Chemical Engineering ATTN: A. Fontijn Troy, NY 12181
1	Stanford University Dept. of Mechanical Engineering ATTN: R. Hanson Stanford, CA 94305
1	University of Texas Dept. of Chemistry ATTN: W. Gardiner Austin, TX 78712
1	University of Utah Dept. of Chemical Engineering ATTN: G. Flandro Salt Lake City, UT 84112
1	Virginia Polytechnic Institute and State University ATTN: J.A. Schetz Blacksburg, VA 24061

DISTRIBUTION LIST

No. Of Copies	Organization
1	Commandant USAFAS ATTN: ATSF-TSM-CN Fort Sill, OK 73503-5600

Aberdeen Proving Ground

Dir, USAMSAA
ATTN: AMXSY-D
AMXSY-MP, H. Cohen
Cdr, USATECOM
ATTN: AMSTE-SI-F
Cdr, CRDC, AMCCOM
ATTN: SMCCR-RSP-A
SMCCR-MU
SMCCR-SPS-IL

USER EVALUATION SHEET/CHANGE OF ADDRESS

This Laboratory undertakes a continuing effort to improve the quality of the reports it publishes. Your comments/answers to the items/questions below will aid us in our efforts.

1. BRL Report Number_____ Date of Report_____

2. Date Report Received_____

3. Does this report satisfy a need? (Comment on purpose, related project, or other area of interest for which the report will be used.)_____

4. How specifically, is the report being used? (Information source, design data, procedure, source of ideas, etc.)_____

5. Has the information in this report led to any quantitative savings as far as man-hours or dollars saved, operating costs avoided or efficiencies achieved, etc? If so, please elaborate._____

6. General Comments. What do you think should be changed to improve future reports? (Indicate changes to organization, technical content, format, etc.)

CURRENT ADDRESS

Name

Organization

Address

City, State, Zip

7. If indicating a Change of Address or Address Correction, please provide the New or Correct Address in Block 6 above and the Old or Incorrect address below.

OLD ADDRESS

Name

Organization

Address

City, State, Zip

(Remove this sheet, fold as indicated, staple or tape closed, and mail.)

FOLD HERE

Director
US Army Ballistic Research Laboratory
ATTN: DRXBR-OD-ST
Aberdeen Proving Ground, MD 21005-5066

NO POSTAGE
NECESSARY
IF MAILED
IN THE
UNITED STATES

OFFICIAL BUSINESS
PENALTY FOR PRIVATE USE. $300

BUSINESS REPLY MAIL
FIRST CLASS PERMIT NO 12062 WASHINGTON, DC
POSTAGE WILL BE PAID BY DEPARTMENT OF THE ARMY

Director
US Army Ballistic Research Laboratory
ATTN: DRXBR-OD-ST
Aberdeen Proving Ground, MD 21005-9989

FOLD HERE

END

FILMED

MARCH, 1988

DTIC